AEROELASTIC GUST – RESPONSE FOR A TYPICAL SECTION WITH SHAPE MEMORY ALLOY (SMA)

Vinícius Piccirillo, pcmec@ita.br
Luiz Carlos Sandoval Goes, goes@ita.br
Roberto Luiz da Cunha Barroso Ramos, rlcbramos@gmail.com
Department of Engineering Aeronautical and Mechanical, Tecnological Institute of Aeronautics – ITA, 12228 – 900, Sao Jose dos Campos, SP, Brazil.

Abstract. *The aeroelastic response to time-dependent external excitation of a two degree of freedom typical airfoil section using a shape memory alloy (SMA) is presented. The expressions of the unsteady aerodynamic lift and moment in the time domain are given in terms of the Wagner's function. In the present investigation, the SMA nonlinearities a concentrated in the airfoil pitch. The effects of the different gust excitations and parameter variations of the SMA element on the aeroelastic response are discussed. The numerical results show the present SMA element can be used to alleviate the dynamic response to a periodic gust excitation, especially for the plunge and pitch responses.*

Keywords*: Aeroelasticity, Shape Memory Alloy, Gust Load, Airfoil Motions.*

1. INTRODUCTION

Shape Memory Alloys (SMA) consist of a group of metallic materials that demonstrate the ability to return to some previously defined shape when they subjected to the appropriate thermal procedure. The shape memory effect occurs due to a temperature and stress dependent shift in the materials crystalline structure between two different phases called martensite and austenite. Martensite, the low temperature phase, is relatively soft whereas austenite, the high temperature phase, is relatively hard. The change that occurs within SMAs crystalline structure it is not a thermodynamically reversible process and results in temperature hysteresis. SMAs have been used in a variety of applications. The dynamical response of the shape memory systems is introduced in different references Bernardini and Vestroni (2003), Savi et. al (2008), Piccirillo et. al. (2009).

Aeroelasticity is the dynamic interaction of structural, inertial, and aerodynamic forces. Conventional methods of examining aeroelastic behavior have relied on a linear approximation of the governing equations which describe both the flow field and the structure. The success of linear flutter analysis is attributed to negligible nonlinear effects, yet aerospace systems inherently contain structural and aerodynamic nonlinearities Dowell et al. (2008) which are critical for many circumstances. Sources of nonlinearities include unsteady aerodynamic sources, aerodynamic stall, large oscillations which lead to flow separation, large deflections of the structure, structural damping mechanisms, and partial loss of structural or control integrity. These aeroelastic systems may exhibit nonlinear dynamic response characteristics such as limit cycle oscillations (LCOs), internal resonances, and chaotic motion, Lee, et.al. (1999).

More recently, aeroelastic modeling has considered the combination of nonlinear and stochastic responses via the inclusion of the effects due to flow random perturbations, as done in (Poirel and Price, 2001). In general, two distinct effects may be identified for an airfoil undergoing a randomly perturbed inflow. In the first case, the perturbation velocity components are orthogonal to the undisturbed flow (vertical gust). In this condition the related aerodynamic forces are independent from the state-space variables (e.g., pitch angle, plunge, modal co-ordinates, etc.) because this perturbation is not coupled with the system behavior and, therefore, its influence is of one-way type. Therefore, the mathematical model describes these forces directly as an external (stochastic) input. In the second case, the perturbation involves only the flow-wise component of the velocity, thus generating aerodynamic forces that are dependent on the state-space variables.

In Dessi and Mastroddi (2008), is analyzed the performed on a simplified aeroelastic model retaining only two structural modes (first bending and first torsional modes) and with a simplified description of both unsteady loads due to wing oscillation and external gust excitation.

Indeed, the inclusion of vertical gust effects in the aeroelastic modeling provides the physical mechanism by which the wing is actually perturbed in the rest condition. This phenomenon has recently been investigated experimentally providing new insight about how the forced wing response combines with the potential onset of LCO in certain flow speed regimes (Tang et al., 2000; Tang and Dowell, 2002). In particular, in the knee-bifurcation scenario, a vertical gust of adequate intensity might induce LCOs of relevant amplitude even below the linear flutter speed.

In Tang et. al. (2004) show a theoretical simulation study of the non-linear gust response of a three degree-of-freedom typical airfoil section with a control surface using an electromagnetic dry friction damper. In this work, we consider the effect of gust loads on the aerodynamics. Sinusoidal and linear frequency sweep gust loads are used. The present results may be helpful in better understanding physically the alleviation of a typical airfoil section response due to gust loads using a shape memory alloy (SMA). We remember that the objective of this study is to illustrate the use of pseudoelastic materials in the passive vibration control.

2. SMA CONSTITUTIVE MODEL

To describe the behavior of the oscillator with shape memory, we adopt in the modeling of the considering problem, the constitutive model proposed by Savi and Braga (1993). This model it is based on Devonshire theory and it defines a free energy of Helmholtz (ψ) in the polynomial form and it is capable to describe the shape memory and pseudoelasticity effects. The polynomial model it is known more to deal with one-dimensional cases and it does not consider an explicit potential of dissipation, and no internal variable is considered. On this form, the free energy depends only on the observable state variables (temperature (T) and strain (ε)), that is, $\psi = \psi(\varepsilon, T)$.

The free energy is defined in such way that, for high temperatures ($T > T_A$), the energy has only one point of minimum corresponding to the null strain representing the stability of the austenite phase (A); for intermediate temperatures ($T_M < T < T_A$) it presents three points of minimum corresponding to the phases austenitic (A), and two other martensitic phase (M^+ and M^-), which are induced by positive and negative stress fields, respectively; in order to low temperature ($T < T_M$) there are two points of minimum representing the two variants of martensite (M^+ and M^-), corresponding the null strain.

Therefore, the restrictions above are given by the following polynomial equation;

$$\rho\psi(\varepsilon, T) = \frac{1}{2}q(T - T_M)\varepsilon^2 - \frac{1}{4}b\varepsilon^4 + \frac{1}{6}e\varepsilon^6 \tag{1}$$

where q and b are constants of the material, T_A correspond to the temperature where the austenite phase it is stable, T_M correspond to the temperature where the martensitic phase it is stable and ρ is the SMA density, and the free energy has only one minimum at zero strain,

$$T_A = T_M + \frac{b^2}{4qe} \tag{2}$$

and the constant e may be expressed in terms of other constants of the material. Thus, the stress-strains relation is given by,

$$\sigma = q(T - T_M)\varepsilon - b\varepsilon^3 + \frac{b^2}{4q(T_A - T_M)}\varepsilon^5 \tag{3}$$

According to Paiva and Savi (2006) the polynomial model represents in a qualitatively coherent way both martensite detwinning process and pseudoelasticity, although it does not consider twinned martensite (M). In other words, there is no stable phase for $T < T_M$ in a stress-free state, but the authors believe that this analysis is useful to the understanding of the nonlinear dynamics of shape memory systems. The proposed model captures itself all of the essential features of the studied phenomenon.

3. EQUATION OF AEROFOIL MOTIONS AND GUST LOAD

Figure 1 shows a sketch of a two-degree-of-freedom (2-dof) airfoil motion in plunge and pitch. The plunge deflection is denoted by h, positive in the downward direction, and α is the pitch angle about the elastic axis, positive nose up. The elastic axis is located at a distance $a_h b$ from the mid-chord, while the mass centre is located at a distance $x_a b$ from the elastic axis, where b is the airfoil semi-chord. Both distances are positive when measured towards the trailing edge of the airfoil.

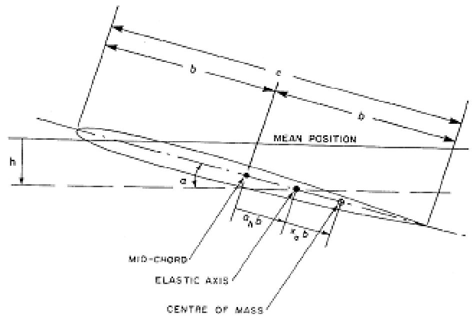

Figure 1: Schematic of airfoil with 2 dof motion

The aeroelastic equations of motion for linear springs have been derived by Fung (1969). For nonlinear SMA restoring forces with subsonic aerodynamics, the coupled bending-torsion equations for the airfoil can be written as follows:

$$mh'' + S_\alpha \alpha'' + K_h h = -C_L + P(t) \tag{4}$$

$$S_\alpha h'' + I_\alpha \alpha'' + K_\alpha \alpha + K_{SMA}(\alpha, T) = C_M + Q(t) \tag{5}$$

where the symbols m, S_α and I_α are the airfoil mass, airfoil static moment about the elastic axis, wing mass moment of inertia about elastic axis, respectively. K_h and K_α are the linear plunge and pitch stiffness terms, and C_L and C_M are the forces and moments acting on the airfoil, respectively and $P(t)$ and $Q(t)$ are the lift and pitch moments due the gust profile, respectively. In this paper we use the polynomial model, and assuming that Eq. 3 is valid for the pure shear stress – strain behavior, Savi and Braga (1993). Note that the restitution force may be expressed as $K_{SMA} = \sigma A$, where A is the area of this SMA element.

Defining

$$\tau = \frac{Ut}{b},\ \xi = \frac{h}{b},\ x_\alpha = \frac{S_\alpha}{bm},\ \omega_\xi^2 = \frac{K_\alpha}{I_\alpha},\ \omega_\alpha^2 = \frac{K_\alpha}{I_\alpha} + \frac{aA(T - T_M)}{I_\alpha},\ r_\alpha^2 = \frac{I_\alpha}{mb^2}\ \ \mu = \frac{m}{\rho b^2 \pi},\ \beta = \frac{bA}{I_\alpha \omega_\xi^2},\ \lambda = \frac{eA}{I_\alpha \omega_\xi^2},$$

the equations (4) and (5) can be written in nondimensional form as follow

$$\ddot{\xi} + x_\alpha \ddot{\alpha} + \left(\frac{\Omega}{V}\right)^2 \xi = P_1(\tau) \tag{6}$$

$$\frac{x_\alpha}{r_\alpha^2} \ddot{\xi} + \ddot{\alpha} + \frac{1}{V^2}\left(\alpha - \beta\alpha^3 + \lambda\alpha^5\right) = Q_1(\tau) \tag{7}$$

In equations (6) and (7), V is a nondimensional velocity defined as $V = \frac{U}{b\omega_\alpha}$ and $\Omega = \frac{\omega_\xi}{\omega_\alpha}$ where ω_ξ and ω_α are the uncoupled plunging and pitching mode natural frequencies, respectively, U is the free-stream velocity, and the dot denotes differentiation with respect to the non-dimensional time τ defined as $\tau = \frac{Ut}{b}$, where

$$P_1(\tau) = \frac{1}{m\mu} C_L(\tau) + \frac{P(\tau) b}{mV^2} \tag{8}$$

$$Q_1(\tau) = \frac{2}{\pi\mu r_\alpha^2} C_M(\tau) + \frac{Q(\tau)}{mV^2 r_\alpha^2} \tag{9}$$

and $\mu = \dfrac{m}{\rho b^2 \pi}$ is the airfoil/air mass ratio For incompressible flow, Fung (1969) gives the following expressions for $C_L(\tau)$ and $C_M(\tau)$.

$$C_L(\tau) = \pi\left(\ddot{\xi} + a_h\ddot{\alpha} + \dot{\alpha}\right) + 2\pi\left\{\alpha(0) + \dot{\xi}(0) + \left(\frac{1}{2} - a_h\right)\dot{\alpha}(0)\right\}\varphi(\tau) + 2\pi\int_0^\tau \varphi(\tau-\sigma)\left(\dot{\alpha}(\sigma) + \ddot{\xi}(\sigma) + \left(\frac{1}{2} - a_h\right)\ddot{\alpha}(\sigma)\right)d\sigma \quad (10)$$

$$\begin{aligned}C_M(\tau) = {} & \pi\left(\frac{1}{2} - a_h\right)\left\{\alpha(0) + \dot{\xi}(0) + \left(\frac{1}{2} - a_h\right)\dot{\alpha}(0)\right\}\varphi(\tau) + \pi\left(\frac{1}{2} - a_h\right)\int_0^\tau \varphi(\tau-\sigma)\left(\dot{\alpha}(\sigma) + \ddot{\xi}(\sigma) + \left(\frac{1}{2} - a_h\right)\ddot{\alpha}(\sigma)\right)d\sigma \\ & + \frac{\pi}{2}a_h\left(\ddot{\xi} - a_h\ddot{\alpha}\right) - \left(\frac{1}{2} - a_h\right)\frac{\pi}{2}\dot{\alpha} - \frac{\pi}{16}\ddot{\alpha}\end{aligned} \quad (11)$$

where the Wagner function $\varphi(\tau)$ is given by

$$\varphi(\tau) = 1 - \psi_1 e^{-\varepsilon_1\tau} - \psi_2 e^{-\varepsilon_2\tau} \quad (12)$$

and the constants $\psi_1 = 0.165$, $\psi_2 = 0.335$, $\varepsilon_1 = 0.0455$ and $\varepsilon_2 = 0.3$ are obtained from Jones (1940).

Atmospheric turbulence creates a gust load that can be represented by two different mathematical descriptions. One is associated with a discrete gust representation usually of a deterministic nature. In the present work, a simple but enlightening hypothesis for the atmospheric (deterministic) gust is sinusoidal. In this case, we write

$$P(\tau) = P_0 \sin(\omega\tau)$$

$$Q(\tau) = Q_0 \sin(\omega_1\tau)$$

and let $F = \dfrac{P_0 b}{mV^2}$ and $F_1 = \dfrac{Q_0}{mV^2 r_\alpha^2}$

so that the second term in equation (8) for $P_1(\tau)$ becomes $F\sin(\omega\tau)$ and in equation (9) becomes $F_1\sin(\omega_1\tau)$. Note the amplitude of gust excitation depends of the aerodynamic and airfoil parameters.

Due to the presence of the integral terms in the integro-differential equations (10) and (11), it is cumbersome to integrate them numerically. A set of simpler equations was derived by Lee et. al. (1999), and they introduced four new variables

$$\begin{aligned} w_1 &= \int_0^\tau e^{-\varepsilon_1(\tau-\sigma)}\alpha(\sigma)d\sigma \quad ; \quad w_2 = \int_0^\tau e^{-\varepsilon_2(\tau-\sigma)}\alpha(\sigma)d\sigma \\ w_3 &= \int_0^\tau e^{-\varepsilon_1(\tau-\sigma)}\xi(\sigma)d\sigma \quad ; \quad w_4 = \int_0^\tau e^{-\varepsilon_2(\tau-\sigma)}\xi(\sigma)d\sigma \end{aligned} \quad (11)$$

equations (6) and (7) can be written as

$$c_0\ddot{\xi} + c_1\ddot{\alpha} + c_2\dot{\xi} + c_3\dot{\alpha} + c_4\xi + c_5\alpha + c_6 w_1 + c_7 w_2 + c_8 w_3 + c_9 w_4 = P_1(\tau) \quad (12)$$

$$d_0\ddot{\xi} + d_1\ddot{\alpha} + d_2\dot{\alpha} + d_3\alpha + d_4\alpha^3 + d_5\alpha^5 + d_6\dot{\xi} + d_7\xi + d_8 w_1 + d_9 w_2 + d_{10} w_3 + d_{11} w_4 = Q_1(\tau) \quad (13)$$

where $P_1(\tau)$ and $Q_1(\tau)$ are functions depending on initial conditions, Wagner's function and the forcing terms, namely,

$$P_1(\tau) = \frac{2}{\mu}\left((0.5 - a_h)\alpha(0) + \xi(0)\right)\left(\psi_1\varepsilon_1 e^{-\varepsilon_1\tau} + \psi_2\varepsilon_2 e^{-\varepsilon_2\tau}\right) + F\sin(\omega\tau)$$

$$Q_1(\tau) = -\frac{(1+2a_h)P_1(\tau)}{2r_\alpha^2} + F_1\sin(\omega_1\tau)$$

The resulting set of eight first-order ordinary differential equations by a suitable transformation is given a

$$\frac{dX}{d\tau} = f(X,\tau) \tag{14}$$

where

$$X = \{x_1,\ x_2,\ \ldots,\ x_8\} = \{\alpha, \dot{\alpha}, \xi, \dot{\xi}, w_1, w_2, w_3, w_4\} \in \Re^8 .$$

Explicitly, the system can be written as

$$\begin{aligned}
\dot{x}_1 &= x_2 \\
\dot{x}_2 &= \frac{1}{c_1d_0 - c_0d_1}(c_0E - d_0F) \\
\dot{x}_3 &= x_4 \\
\dot{x}_4 &= \frac{1}{c_1d_0 - c_0d_1}(-c_1E + d_1F) \\
\dot{x}_5 &= x_1 - \varepsilon_1x_5 \\
\dot{x}_6 &= x_1 - \varepsilon_2x_6 \\
\dot{x}_7 &= x_3 - \varepsilon_1x_7 \\
\dot{x}_8 &= x_3 - \varepsilon_2x_8
\end{aligned}$$

where

$$\begin{aligned}
E &= -Q_1(\tau) + d_2x_2 + d_3x_1 + d_4x_1^3 + d_5x_1^5 + d_6x_4 + d_7x_3 + d_8x_5 + d_9x_6 + d_{10}x_7 + d_{11}x_8 \\
F &= P_1(\tau) + c_2x_4 + c_3x_2 + c_4x_3 + c_5x_1 + c_6x_5 + c_7x_6 + c_8x_7 + c_9x_8
\end{aligned}$$

and

$$c_0 = 1+\frac{1}{\mu}, c_1 = x_\alpha - \frac{a_h}{\mu}, c_2 = \frac{2}{\mu}(1-\psi_1-\psi_2), c_3 = \frac{1+2(0.5-a_h)(1-\psi_1-\psi_2)}{\mu}, c_4 = \left(\frac{\Omega}{V}\right)^2 + \frac{2}{\mu}(\psi_1\varepsilon_1+\psi_2\varepsilon_2),$$

$$c_5 = \frac{2}{\mu}\{(1-\psi_1-\psi_2)+(0.5-a_h)(\psi_1\varepsilon_1+\psi_2\varepsilon_2)\}, c_6 = \frac{2}{\mu}\psi_1\varepsilon_1\{1-(0.5-a_h)\varepsilon_1\}, c_7 = \frac{2}{\mu}\psi_2\varepsilon_2\{1-(0.5-a_h)\varepsilon_2\},$$

$$c_8 = -\frac{2}{\mu}\psi_1\varepsilon_1^2, c_9 = -\frac{2}{\mu}\psi_2\varepsilon_2^2$$

$$d_0 = \frac{x_\alpha}{r_\alpha^2} - \frac{a_h}{\mu r_\alpha^2}, d_1 = 1+\frac{1+8a_h^2}{8\mu r_\alpha^2}, d_2 = \frac{1-2a_h}{2\mu r_\alpha^2} - \frac{(1+2a_h)(1-2a_h)(1-\psi_1-\psi_2)}{2\mu r_\alpha^2},$$

$$d_3 = \frac{1}{V^2} - \frac{1+2a_h}{2\mu r_\alpha^2} - \frac{(1+2a_h)(1-2a_h)(\psi_1\varepsilon_1+\psi_2\varepsilon_2)}{2\mu r_\alpha^2}, d_4 = -\frac{\beta}{V^2}, d_5 = \frac{\lambda}{V^2}, d_6 = \frac{-(1+2a_h)(1-\psi_1-\psi_2)}{\mu r_\alpha^2},$$

$$d_7 = \frac{-(1+2a_h)(\psi_1\varepsilon_1+\psi_2\varepsilon_2)}{\mu r_\alpha^2}, d_8 = \frac{-(1+2a_h)\psi_1\varepsilon_1\left[1-(0.5-a_h)\varepsilon_1\right]}{\mu r_\alpha^2}, d_9 = \frac{-(1+2a_h)\psi_2\varepsilon_2\left[1-(0.5-a_h)\varepsilon_2\right]}{\mu r_\alpha^2},$$

$$d_{10} = \frac{(1+2a_h)\psi_1\varepsilon_1^2}{\mu r_\alpha^2}, d_{11} = \frac{(1+2a_h)\psi_2\varepsilon_2^2}{\mu r_\alpha^2}$$

4. V-g METHOD FOR LINEAR FLUTTER ANALYSIS

Let's express the above flutter equation in the following matrix form.

$$\left[K_{ij}\right]\begin{Bmatrix} \frac{`h}{b} \\ \alpha \end{Bmatrix} = \Omega^2\left[A_{ij}+M_{ij}\right]\begin{Bmatrix} \frac{`h}{b} \\ \alpha \end{Bmatrix} \tag{15}$$

where K_{ij} is the stiffness matrix, M_{ij} mass matrix, and A_{ij} is the aerodynamic matrix. Note that the aerodynamic matrix is function of the reduced frequency, k . V-g method assumes first the artificial structural damping, g.

This artificial damping indicates the required damping for the harmonic motion. The eigenvalues of the equation of motion represent a point on the flutter boundary if the corresponding value of g equals the assumed value of g**.**

For give reduced frequency, $k = \frac{\omega b}{V}$, it is a complex eigenvalue problem.

$$\frac{(1+ig)}{\Omega^2}\left[K_{ij}\right]\begin{Bmatrix} \frac{`h}{b} \\ \alpha \end{Bmatrix} = \left[A_{ij}+M_{ij}\right]\begin{Bmatrix} \frac{`h}{b} \\ \alpha \end{Bmatrix} \tag{16}$$

The eigenvalue is $\lambda = \frac{1+ig}{\Omega^2}$. From this eigenvalue we have $\frac{1}{\lambda_{Re}} = \frac{\omega_i^2}{\omega_\theta^2}$, $g = \frac{\lambda_{Im}}{\lambda_{Re}}$

The complex eigenvalue problem is solved beginning with large values of k and then decreasing k until a flutter velocity is found. If there is no actual damping in the system, when the artificial damping, g , first becomes positive, flutter will occur.

Figure 2 show the frequency$\left(\frac{\omega}{\omega_\theta}\right)$, damping of the reduced order model against the reduced velocity $\left(\frac{V}{\omega_\theta b}\right)$. In V-g method, the unsteady aerodynamics formulated by Wagner is used. The flutter speed calculated using V-g method is about 4.5, i.e., the critical flutter velocity is approximately $U = 28.6m/s$. Note that the frequency and g from V-g method do not have the physical meaning except at the flutter speed. On the other hand, the value of g obtained from the current method denotes the real damping of the system at the specified airspeed. That is identical with the flutter speed using the current formulation.

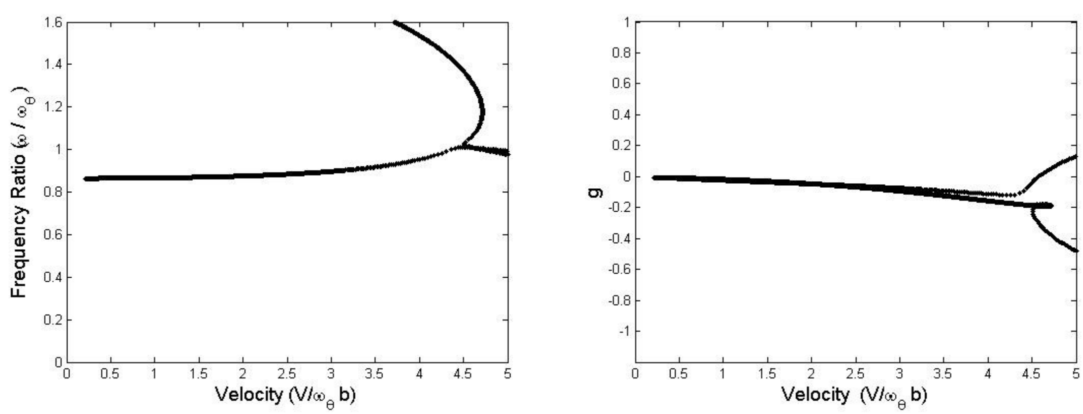

Figure 2: Linear Flutter Result: (a) Frequency vs Velocity and (b) g vs velocity

5. NUMERICAL ANALYSIS

Usually, the physical mechanism that makes the wing to vibrate is due to airplane maneuvering and/or to gust occurrence. The numerical simulations are obtained by a fourth-order Runge-Kutta algorithm. Now, we introduce in pitch the SMA spring. This model is used to investigate the effect of the nonlinearity in this aeroelastic system. In this case we used a temperature of the alloy around $T = 323K$ approximately $T \approx 50°C$. The initial torsion displacement is chosen to be 0.3° unless otherwise noted. The flow velocity is chosen as $U = 18 m/s$, lower than the flutter velocity. The parameters of aerofoil used in this work are described in Tang et. al. (2004) and present in table 1.

Table 1. System parameters of two-dimensional typical section model

Span (l)	0.52 m
Semi – chord (b)	0.127
Elastic axis (a)	-0.0625 m
Mass of wing	0.713 kg
I_α (per span)	0.0185 kg m
S_α (per span)	0.0726 kg
K_α (per span)	42.8 kg m/s^2
K_h (per span)	2755.4 kg m / s^2

As the shape memory alloys presents different properties, depending on the temperature, in this paper, we present a study on the pseudoelastic dynamic behavior, considering a higher temperature, where austenitic phase is stable in the alloy. In all simulations, to analyze the behavior of the aeroelastic dynamical system, where the spring is assumed to be made of a Ni-Ti alloy and the properties are present in Table 2 (Paiva and Savi, 2006).

Table 2. Material constants for a Ni-Ti alloy

Parameter	Units	Values
q	MPa/K	1000
b	Mpa	40×10^6
T_M	K	287
T_A	K	313

We assume that the gust loads are sinusoidal and without loss in generality, the gust is only applied in the pitch degree of freedom. In this case $P(\tau) = 0$. The results are shown in Figure 3 for the plunge and pitch amplitude versus the gust excitation frequency (amplitude frequency curves). The curves were obtained by allowing the system to achieve steady-state motion, while the gust excitation frequency was fixed. Then, the amplitude of the steady-state response was measured. The curve was calculated, using an increment $\Delta\omega_1 = 0.005$, as the variation of the parameter ω_1 in the interval [0, 2] and holding in the new position until a new steady state was achieved. Both set of figures show the presence of two peaks at approximately 0.325 and 0.48. These frequencies can be estimated from Eqs. (12) and (13). As shown in Fig. 3(a) when no SMA element is included in the system, the pitch resonance amplitude is 1.452. When we include the SMA spring in this system the amplitude decreases to 0.1871. Note at this figure, that in the frequency interval [0.515, 0.635] the SMA response is bigger amplitude than linear system, this occur due to nonlinearities presents in SMA.

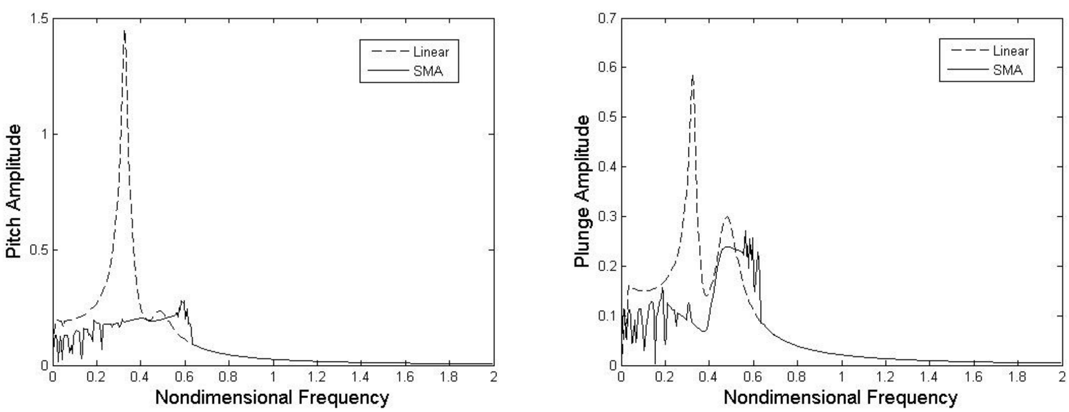

(a) (b)

Figure 3: Frequency response curves: (a) Pitch and (b) Plunge motions

In Fig. 3(b) shown the linear plunge resonance amplitude is 0.5875, but when include the SMA spring in pitch d.o.f. the amplitude decreases to 0.08434. Note in this case the system present a second peak of resonance. In this case the SMA also reduces the amplitude of the response. However, in the SMA case the system present a bigger response than linear system due again the nonlinearities introduced in the wing section.

The next figure shows the pitch and plunge time history at nondimensional frequency 0.325. This frequency represents the worst case, that is, in this case the system presents the bigger peak of resonance in linear system. Fig. 4(a) shows the time history for the pitch motion and the Fig. 4(b) show the plunge behavior. Note, that in both case, the SMA element reduces significant the amplitude of the motion.

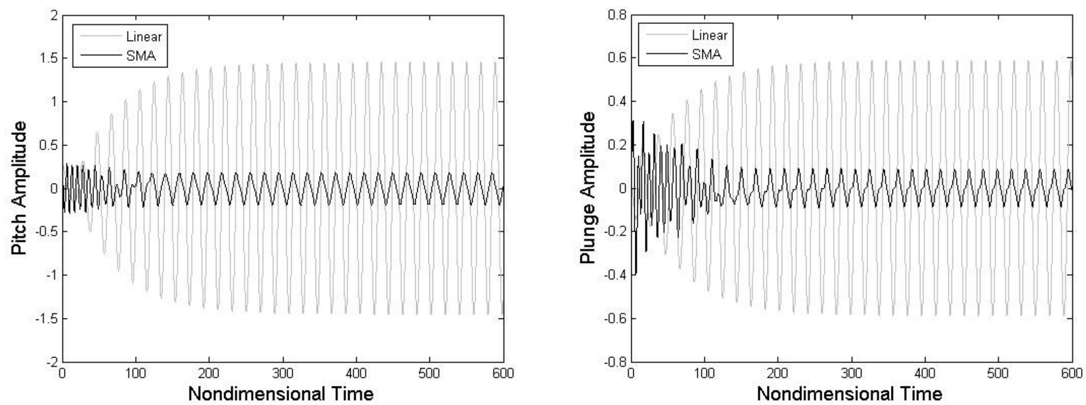

(a) (b)

Figure 4: Time history behavior: (a) Pitch and (b) Plunge response for $\omega = 0.325$

The theoretical lateral peak gust angle of attack is chosen to be 0.3º for a continuous linear frequency sweep gust load. The minimum and maximum frequencies are 0 and 2.5; and the sweep duration T is 1000 nondimensional time. The initial conditions are set to zero for all time simulations. Firstly, linear system results are examined without the SMA element. The results are shown in Fig. 5. The effects of the SMA spring on the gust response are also considered in the sweep frequency gust. In Fig. 6 show the response the same sweep gust load but now we include the SMA spring in pitch d.o.f. Comparing the Figs. 5 and 6, we observed that the plunge and pitch gust responses significantly decrease as the temperature imposed in the system.

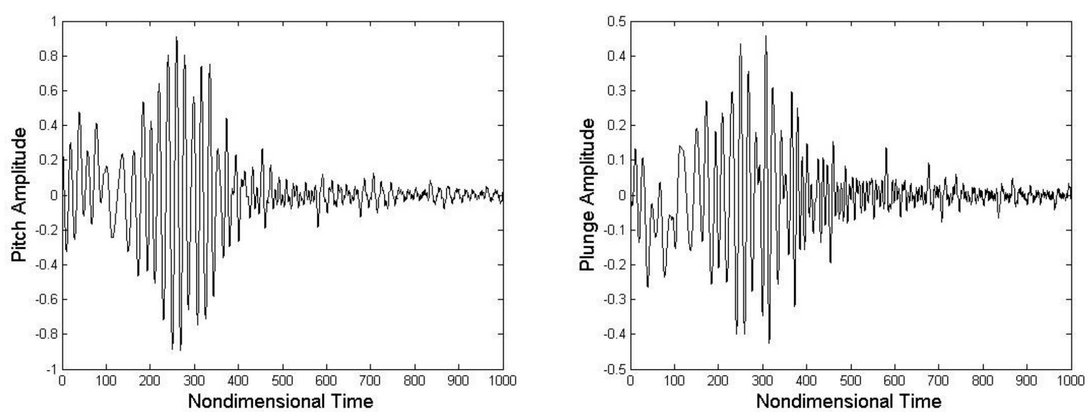

(a) (b)

Figure 5: Gust linear response to a sweep frequency: (a) Pitch and (b) Plunge linear behavior

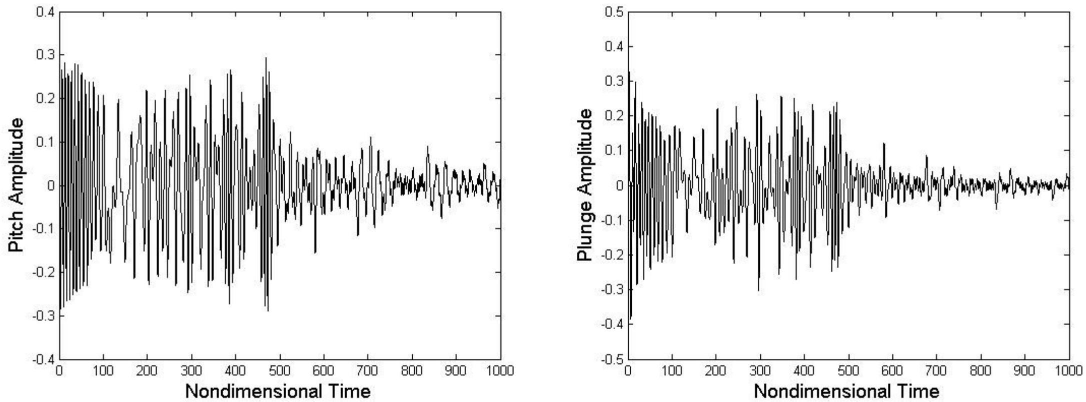

(a) (b)

Figure 6: Gust linear response to a sweep frequency: (a) Pitch and (b) Plunge SMA behavior

5. CONCLUSION

This paper, analyzed the influence of the SMA element on an aeroelastic vibrating system. We present the study on the pseudoelastic behavior, considering a higher temperature, where austenitic phase is stable in the alloy.

We introduce the SMA in pitch d.o.f with the intention to increase the rigidity in torsion, and thus to be able uses it as a form of dependent control of the temperature.

An SMA controllable through temperature has been designed and numerically simulated. The non-linear gust response of a two d.o.f. typical airfoil section using this nonlinear element has been studied theoretically. Results for both a periodic and a linear frequency sweep gust excitations show that the present SMA element can be used to alleviate the gust response, especially for the plunge and pitch responses.

This show that the SMA is sufficiently efficient in the solution of this kind of problem, carrying through well it task with one passive control device. This is a first use of this kind of control on aeroelastic vibrating system.

6. ACKNOWLEDGEMENTS

The authors thank the support of the Brazilian government Agency CNPq.

7. REFERENCES

Bernardini, D., Vestroni, F., 2003, “Non-isothermal Oscillations of Pseudoelastic Devices”, International Journal of Nonlinear Mechanics, Vol. 38, pp. 1297 – 1313.

Dessi, D., Mastroddi, F., 2008, “A Nonlinear Analysis of Stability and Gust Response of Aeroelastic System”, Journal of Fluids and Structures, Vol. 24, pp. 436 – 445.

Dowell, E.H., Crawley, E.F., Curtiss Jr., Peters, D.A., H.C., Scanlan, R.H., Sisto, F., 2008, “A Modern Course in Aeroelasticity”, Ed. Springer-Verlag, New York, USA, pp.746.

Fung, Y.C., 1969, “An Introduction to the Theory of Aeroelasticity”, Dover, New York, pp.498.

Jones, R.T., 1940, “The Unsteady Lift of a Wing of Finite Aspect Ratio”, NACA Report 681.

Lee, B.H.K., Price, S.J., Wong, Y.S., 1999, “Nonlinear Aeroelastic Analysis of Airfoil: Bifurcations and Chaos”, Progress in Aeroespace Science, Vol. 35, pp. 205 – 334.

Paiva, A., Savi, M.A., 2006, “An Overview of Constitutive Models for Shape Memory Alloy”, Mathematical Problem in Engineering, Vol. 2006, pp. 1 – 30.

Piccirillo, V., Balthazar, J.M., Pontes Jr., B.R. and Felix, J.L.P., 2009, “Control of a Nonlinear Oscillator with Shape Memory Alloy Using an Optimal Linear Control: Part I: Ideal Energy Source”, Nonlinear Dynamics, Vol. 55, pp. 139 – 149.

Poirel, D.C., Price, S.J., 2001, “Structurally Nonlinear Fluttering Airfoil in Turbulent Flow”. AIAA Journal 39, Vol. 10, pp.1960–1968.

Savi, M., and Braga, A.M.B., 1993, “Chaotic Vibrations of an Oscillator with Shape Memory”, Journal of the Brazilian Society of Mechanical Sciences and Engineering, Vol. XV, pp. 1 – 20.

Savi, M., Sá, M.A.N., Paiva, A. and Pacheco, P.M.C.L., 2008, “Tensile-Compressive Asymmetry Influence on Shape Memory Alloy System Dynamics”, Chaos, Solitons & Fractal, Vol 36, pp. 828 – 842.

Tang, D., Henry, J.K., Dowell, E.H., 2000. “Nonlinear Aeroelastic Response of Delta Wing to Periodic Gust”, Journal of Aircraft 37 Vol. 1, pp. 155–164.

Tang, D., Dowell, E.H., 2002. "Experimental and Theoretical Study of Gust Response for High-Aspect-Ratio Wing". AIAA Journal 40, Vol. 3, pp. 419–429.

Tang, D., Henri, P.G., Dowell, E.H., 2004, "Study of Airfoil Gust Response Alleviation Using an Electro-Magnetic Dry Friction Damper. Part 1: Theory", Journal of Sound and Vibration, Vol. 269, pp. 853 – 874.

5. RESPONSIBILITY NOTICE

The authors are the only responsible for the printed material included in this paper.